Exosomes derived from endoplasmic reticulum-stressed liver cancer cells enhance the expression of cytokines in macrophages via the STAT3 signaling pathway

CHENGQUN HE[1,2], WEI HUA[3], JIATAO LIU[1,3], LULU FAN[1], HUA WANG[1,4] and GUOPING SUN[1]

[1]Department of Oncology, The First Affiliated Hospital of Anhui Medical University, Hefei, Anhui 230022;
[2]Department of Gynecological Oncology, Anhui Province Hospital, Hefei, Anhui 230032;
[3]Department of Pharmacy, The First Affiliated Hospital of Anhui Medical University;
[4]Department of Liver Cancer, Institute for Liver Diseases of Anhui Medical University, Hefei, Anhui 230022, P.R. China

Received May 5, 2019; Accepted April 1, 2020

DOI: 10.3892/ol.2020.11609

Abstract. Previous studies have shown that endoplasmic reticulum (ER) stress serves an important role in shaping the immunosuppressive microenvironment by modulating resident immune cells. However, the communication between ER-stressed tumor cells and immune cells is not fully understood. Exosomes have been reported to play a vital role in intercellular communication. Therefore, in order to investigate the role of ER stress-related exosomes in liver cancer cells mediated macrophage function remodeling, immunohistochemical analysis, western-blotting immunofluorescence and cytokine bead array analyses were performed. The results demonstrated that glucose-regulated protein 78 (GRP78) expression was upregulated in human liver cancer tissue. Moreover, 69.09% of GRP78-positive liver cancer tissues possessed macrophages expressing $CD68^+$ ($r=0.55$; $P<0.001$). In addition to these $CD68^+$ macrophages, interleukin (IL)-10 and IL-6 expression levels were increased in liver cancer tissues. It was also demonstrated that exosomes released by ER-stressed HepG2 cells significantly enhanced the expression levels of several cytokines, including IL-6, monocyte chemotactic protein-1, IL-10 and tumor necrosis factor-α in macrophages. Furthermore, incubation of cells with ER stress-associated exosomes resulted inactivation of the Janus kinase 2/STAT3 pathway, and inhibition of STAT3 using S3I-201 in RAW264.7 cells significantly reduced cytokine production. Collectively, the present study identified a novel function of ER stress-associated exosomes in mediating macrophage cytokine secretion in the liver cancer microenvironment, and also indicated the potential of treating liver cancer via an ER stress-exosomal-STAT3 pathway.

Correspondence to: Dr Guoping Sun, Department of Oncology, The First Affiliated Hospital of Anhui Medical University, 218 Jixi Road, Hefei, Anhui 230022, P.R. China
E-mail: sungp@ahmu.edu.cn

Key words: liver cancer, endoplasmic reticulum stress, macrophage, exosome, inflammation

Introduction

Liver cancer is a common malignant tumor, which was reported to account for ~8.2% of cancer-associated mortality globally in 2018 (1,2). Escaping immunological surveillance has been extensively investigated in liver cancer in the past decade (3); however, the precise mechanisms remain unknown. Therefore, determining the molecular mechanisms contributing to immune escape in liver cancer cells, and identifying specific therapeutic targets, require further examination; which will improve the efficacy of immunotherapy and the development of novel immunotherapeutics.

Endoplasmic reticulum (ER) homeostasis is a basic condition for cell survival; however, in a hostile tumor microenvironment (TME), tumor cells frequently experience glucose and oxygen deprivation, oxidative stress and loss of Ca^{2+} homeostasis, which collectively contribute to the production and accumulation of incompletely or incorrectly folded proteins in the lumen of the ER (4). Moreover, the accumulation of misfolded proteins results in ER dysfunction, and thus, the cell enters a cellular state termed 'ER stress' in order to maintain cell survival (5,6). Mild and chronic upregulation of ER-stress activity enables malignant cells to exhibit several aggressive characteristics, such as invasion, metastasis and apoptotic-resistance (7). Furthermore, previous studies have shown that ER stress may disrupt anti-tumor immunity by modulating the role of tumor-associated macrophages (TAMs) residing in the TME (8,9). In addition, the intercellular interaction between ER-stressed tumor cells and resident immune cells in the TME has gained attention in several different types of cancer, for example liver cancer (10,11). However, the mediators linking these two types of cells are not yet fully understood.

Exosomes are a class of extracellular vesicles, possessing a double-layer membrane structure, that are secreted by almost all cell types and play a vital role in cell-to-cell

communication by acting as carriers of cell soluble proteins, lipids and RNA (12,13). Exosomes released by tumor cells are enriched in immunosuppressive molecules, as well as biologically-active soluble factors, which may interact with immunological effector cells in the TME, leading to the dysfunction of anti-tumor immunity by delivering immunosuppressive signal (14,15). By suppressing the functions of immunological effector cells, tumor-derived exosomes promote tumor progression and facilitate tumor cell escape from immunological surveillance (16,17). Moreover, Chen *et al* (16) reported that exosomes released from hypoxic epithelial ovarian cancer cells deliver a range of microRNAs (miRNAs) to macrophages, and can remodel macrophages into an oncogenic phenotype to promote tumor cell proliferation and migration. However, whether exosome releasing from ER stressed liver cancer cells is capable of immunosuppression remains to be determined.

Therefore, the present study investigated the role of exosomes, released from ER-stressed liver cancer cells, on macrophage function. Furthermore, it was demonstrated that ER stress-associated exosomes increased cytokine production via the STAT3 pathway in macrophages.

Materials and methods

Cell culture. The human liver cancer cell line HepG2 (authenticated using short tandem repeat profiling) and the murine macrophage cell line RAW264.7 were purchased from The Cell Bank of Type Culture Collection of the Chinese Academy of Sciences. Cells were cultured in DMEM (Thermo Fisher Scientific, Inc.) containing 10% heat-inactivated FBS (Thermo Fisher Scientific, Inc.) at 37˚C in a humidified 5% CO_2 atmosphere.

Exosomes isolation. HepG2 cells were cultured in DMEM media containing 10% exosome-free FBS (System Biosciences, LLC) up to a confluence of 80%. Exosomes from the supernatants of normal cultured HepG2 cells (Exo-con) and HepG2 cells treated with 2.5 μM tunicamycin (Sigma-Aldrich; Merck KGaA) (Exo-TM) at 37˚C for 24 h were purified using ExoQuick Precipitation Solution (System Biosciences, LLC) at the volume ratio of 1:5, according to the manufacturer's protocol. Supernatants of the Exo-con group and the Exo-TM group were collected and centrifuged at 3,000 x g for 15 min at room temperature to remove cell debris. ExoQuick precipitation solution was added to the centrifuged supernatant at a ratio of 1:5 (v/v), agitated and incubated at 4˚C for 12 h. After incubation, the mixture was centrifuged at 3,000 x g for 30 min at 4˚C, and the supernatants were removed and discarded. The pellet was centrifuged under the same conditions to remove excess fluid. Then, the plates (collected exosome mass) were washed twice with sterile PBS. Protein quantification of exosome preparations was measured using a bicinchoninic acid assay kit (Beyotime Institute of Biotechnology).

Transmission electron microscopy (TEM). The morphology and size of Exo-con and Exo-TM was measured using TEM (JEM-1230; Jeol Ltd.). Exosomes were stored at -80˚C and thawed on ice when required. Then, 10 μl suspension liquid (sterile PBS) was added onto the formvar carbon-coated copper grids and the excess liquid was absorbed using a filter paper. Subsequently, 30 μl 2% phosphotungstic acid was added to the copper net to negatively stain exosomes at room temperature for 5 min, and the excess liquid was removed using filter paper. The grids were washed with PBS three times and dried under an incandescent lamp. Representative exosome images were captured using TEM.

Construction of tissue microarray (TMA). TMA was constructed as previously reported (18). Formalin-fixed (using 4% paraformaldehyde at room temperature for 24 h) and paraffin-embedded liver cancer tumor tissues and paired healthy liver tissues were obtained from the Department of Pathology of The First Affiliated Hospital of Anhui Medical University between March 2004 and July 2010 as previously. A total of 89 patients were included in this study (21 women and 68 men; age range, 28-76 years; mean ± standard deviation, 51.0±12.3 years). To identify the target area for construction of TMAs, the 4-μm-thick specimen sections were analyzed using 0.5% hematoxylin and eosin-staining at room temperature for 1 min. Then, five representative 1-mm cores (three tumor tissues and two paired healthy tissues) were obtained from each patient and marked tissues were embedded into a new blank paraffin block according to the design grid using a manual tissue arrayer (Nantong Hengtai Graphite Equipment Systems Co., Ltd., http://www.smlnq.com/en/index.asp).

Immunohistochemical analysis. The primary hepatocellular carcinoma (HCC) tumor tissues used were the same as used in a previous study (18). The protocol of the current study conforms to the Ethical Guidelines of the 1975 Declaration of Helsinki and was approved by the Ethics Committee of The First Affiliated Hospital of Anhui Medical University (approval no. 20040158). Written consent was provided by all the enrolled patients. Sections (thickness, 4 μm) were deparaffinized and 3% hydrogen peroxide in methanol was used to block endogenous peroxidase activity at room temperature for 10 min. The slides were placed into heated (96-98˚C) sodium citrate buffer (0.01 M; pH=6.0) for 15 min for antigen retrieval and allowed to cool at room temperature. Incubation with 5% BSA blocking solution (Beyotime Institute of Biotechnology) was performed for 20 min to block non-specific binding at room temperature. The sections were subsequently incubated with primary antibodies, including glucose-regulated protein 78 (GRP78; cat. no. ab108615; Abcam), CD68 (cat. no. ab955; Abcam), IL-6 (cat. no. ab9324; Abcam) and IL-10 (cat. no. ab34843; Abcam) in a moist chamber at 4˚C overnight; all primary antibodies were diluted at 1:200. After incubation, PBS was used to wash the sections, which were then incubated with a biotinylated secondary antibody (1:5,000; cat. no. BA1004; Wuhan Boster Biological Technology, Ltd.) and peroxidase-conjugated streptavidin (cat. no. BA1088; Wuhan Boster Biological Technology, Ltd.) at room temperature for 15-20 min. TMA sections were stained with 1% diaminobenzidine solution for 1 min and counterstained using 0.5% hematoxylin for 30 sec at room temperature, respectively. The binding of target antigen was observed under an optical light Olympus microscope (magnification, x100 and x400).

The expression of GRP78 was scored by multiplying the staining intensity (0 for negative staining; 1 for light yellow;

2 for orange-brown and 3 for brown) with the percentage of stained cells (0 for negative; 1 for ≤10%; 2 for 11-50%; 3 for 51-75%; and 4 for >75%). Moreover, the product <5 and ≥5 indicated low and high expression levels of GRP78 and the product between 3-5 was grouped as medium expression (18). CD68, interleukin (IL)-6 and IL-10 distribution was scored by counting the mean percentage of positive cells in five random fields of each sample.

Western blotting. Total cellular and exosomal proteins were lysed using RIPA buffer (Beyotime Institute of Biotechnology) with 1 nM PMSF, quantified with a bicinchoninic acid assay, and then ~20 μg of total proteins were loaded per lane and resolved on 10% gels using SDS-PAGE. Proteins were transferred onto PVDF membranes (EMD Millipore) and blocked with 5% non-fat milk at room temperature for 2 h. The membranes were washed three times with Tris Buffered saline Tween solution and then incubated with the following primary antibodies: Mouse anti-β-actin (cat. no. 3700; Cell Signaling Technology, Inc.), rabbit anti-CD63 (cat. no. ab217345; Abcam), rabbit anti-CD81 (cat. no. ab109201; Abcam), rabbit anti-tumor susceptibility gene 101 (TSG101; cat. no. ab125011; Abcam), rabbit anti-Calnexin (cat. no. 2679; Cell Signaling Technology, Inc.), rabbit anti-Janus kinase 2 (JAK2; cat. no. ab108596; Abcam), rabbit anti-phosphorylated (p)-JAK2 (cat. no. ab32101; Abcam), rabbit anti-STAT3 (cat. no. ab119352; Abcam), rabbit anti-p-STAT3 (cat. no. ab76315; Abcam) and rabbit anti-GRP78 (cat. no. BS1154; Biogot Technology Co., Ltd.) at 4˚C overnight; all primary antibodies were diluted at 1:1,000. Horseradish peroxidase-labeled anti-mouse (cat. no. BS12478) or anti-rabbit (cat. no. BS13278) immunoglobulin G (both Biogot Technology Co., Ltd.) were used as the secondary antibodies at a dilution of 1:10,000 for 2 h at 37˚C. The bands were visualized using SuperSignal West Dura (Thermo Fisher Scientific, Inc.) and the intensity of the bands were semi-quantitative analyzed using Scion Image software (version 4.0.3.2; http://softwaretopic.informer.com/search-scion-image).

Immunofluorescence. To detect macrophages that had incorporated exosomes, RAW264.7 cells were co-cultured with PKH67- (Sigma-Aldrich; Merck-KGaA) labeled exosomes for 12 h at 37˚C, and subsequently fixed with 4% formaldehyde for 30 min at 37˚C and permeabilized with 0.1% Triton-X. Cells were imaged using a confocal microscope (Leica Microsystems GmbH; magnification, x100) after counter-staining cells with DAPI (1 mg/ml) at room temperature for 5 min.

To detect the expression levels of IL-6 and IL-10 in CD68-positive cells, the sections were prepared as described for immunohistochemistry and incubated at 4˚C overnight with mouse anti-CD68 (1:200; cat. no. ab955; Abcam), rabbit anti-IL-10 (1:200; cat. no. ab34843; Abcam;) or rabbit anti-IL-6 (1:200; cat. no. ab9324; Abcam) and goat anti-mouse IgG (H+L) unconjugated or goat anti-rabbit IgG (H+L) unconjugated secondary antibodies (1:5,000; cat. nos. BS13271 and BS12471; Biogot Technology Co., Ltd.) for 2 h at 37˚C. Cells were counter-stained with DAPI (100 ng/ml) for 5 min at room temperature. Co-localization of CD68 with IL-6 or IL-10 was determined using an Olympus fluorescence microscope (magnification, x100).

Cytokine bead array (CBA) analyses of inflammatory factors. RAW264.7 cells were co-cultured with Exo-con and Exo-TM for 24 h at 37˚C, then the culture supernatants were collected to detect the expression levels of IL-10, IL-6, monocyte chemo-attractant protein-1 (MCP-1) and tumor necrosis factor-α (TNF-α). The aforementioned inflammatory factors were measured using a mouse CBA kit (cat. no. 552364; BD Biosciences), according to the manufacturer's protocol.

Statistical analysis. SPSS version 16.0 software (IBM Corp.) was used for statistical analysis. Data are presented as the mean ± SD of ≥3 independent experiments. Kaplan-Meier analysis was performed to determine the association between GRP78 expression and overall survival (OS) time of patients with liver cancer and log-rank test was used to determine statistical significance, while Spearman's rank correlation analysis was performed to assess the association between IL-10 and IL-6. The association between GRP78 expression levels and clinicopathological characteristics was determined using the χ^2 test or Mann-Whitney test. A paired t-test was used for comparison between two groups, and a one-way ANOVA followed by Tukey's test post hoc test was used for comparing ≥3 groups. $P<0.05$ was considered to indicate a statistically significant difference.

Results

Activation of ER stress is associated with poor prognosis in patients with liver cancer. To determine whether ER stress was increased in liver cancer tissues, the expression of GRP78, an ER stress biomarker, was measured in 89 paraffin-embedded liver cancer specimens using immunohistochemical staining. It was found that GRP78 protein expression was primarily located in the cytoplasm in a diffuse pattern (Fig. 1A). Of the 89 liver cancer specimens, 61.80% (55/89) of tissues stained positive for GRP78 (Fig. 1B). Moreover, GRP78 protein expression was also measured by western blotting in three freshly resected liver cancer tissues, and it was demonstrated that GRP78 expression was higher in tumor tissues compared with the paired healthy liver tissues (Fig. 1C and D). Furthermore, the association between clinicopathological characteristics and GRP78 expression in patients with liver cancer is shown in Table I. The results indicated that GRP78 expression was associated with hepatitis, cirrhosis, larger tumor size and poor differentiation (Table I). In addition, Kaplan-Meier analysis was used to analyze the association of GRP78 expression with overall survival (OS) time of 35 patients with liver cancer. It was identified that patients with lower expression levels of GPR78 had a significantly longer OS time compared with patients with higher expression levels of GPR78 (Fig. 1E).

Activation of ER stress is associated with macrophage recruitment and cytokines secretion. TAMs serve a vital role in liver cancer progression (19). Therefore, to investigate whether upregulation of ER stress activity is associated with macrophage recruitment, the expression of the macrophage surface marker CD68 was determined in liver cancer tissues. The results suggested that CD68-positive cells were distributed sporadically in tissues with low GRP78 expression, whereas the number of CD68-positive cells was higher and cells were

Table I. Association between clinicopathological features and GRP78 expression in patients with hepatocellular carcinoma.

Clinicopathological features	GRP78 expression				
	Case (n)	Low (n)	High (n)	$\chi^{2/Z}$	P-value
Sex				6.541	0.019[a]
Female	21	13	8		
Male	68	21	47	0.234	0.665
Age, years					
<60	50	18	32		
≥60	39	16	23		
Hepatitis				6.75	0.013[a]
No	23	14	9		
Yes	66	20	46		
Cirrhosis				6.773	0.016[a]
No	42	22	20		
Yes	47	12	35		
AFP value				-0.317	0.751
<20	39	16	23		
≥20, <400	21	7	14		
≥400	29	11	18		
Clinical stages				1.136	0.333
I/II	65	27	38		
III/IV	24	7	17		
Tumor size				-2.024	0.043[a]
<5	29	15	14		
≥5, <10	46	16	30		
≥10	14	3	11		
Differentiated degree				-2.664	0.008[a]
High	18	17	15		
Middle	50	16	29		
Low	18	1	11		

[a]P<0.05. GRP78, glucose-regulated protein 78; AFP, alpha-fetoprotein.

present in clusters in tissues with GRP78-high expression (Fig. 2A).

Furthermore, the association between the expression levels of GRP78 and IL-10 and IL-6 in infiltrating macrophages was assessed using immunohistochemical staining. Both low and high GRP78 expressing liver cancer tissues stained positively for IL-10 and IL-6, and higher GRP78 expressing tissues secreted increased quantities of IL-10 and IL-6 (Fig. 2B). As macrophages produce various cytokines including IL-10 and IL-6 (18,19), the expression levels of these cytokines were determined in $CD68^+$ macrophages in liver cancer tissues using double immunofluorescence staining of CD68/IL-6 (Fig. 2C) and CD68/IL-10 (Fig. 2D). The results demonstrated that tissues overexpressed GRP78 protein frequently infiltrating large number of macrophages, and these macrophages expressed higher levels of IL-10 and lower levels of IL-6 than those macrophages resided in HCC tissues that expressed lower levels of GRP78 protein. Thus, these results suggest that the activation of ER stress may be correlated with macrophages infiltration and cytokines secretion in liver cancer, and macrophages were identified as an important group of immunosuppressive cells in liver cancer.

Exosomes released from ER-stressed liver cancer cells increase cytokine expression. To investigate whether ER stress-associated exosomes affected cytokine expression in macrophages, HepG2 cells were co-cultured using different concentrations of TM for 24 h, and the GRP78 protein expression was detected using rabbit anti-GRP78. It was found that the expression of GRP78 was increased in a concentration-dependent manner and peaked when cells were incubated with 2.5 μM TM (Fig. 3A and B). HepG2 cells were also treated with 2.5 μM TM for 12, 24 and 48 h, and GRP78 expression was increased in a time-dependent manner, although it appears that 48 h has a slightly higher expression level of GRP78 proteins than 24 h, there was no significant difference between 24 and 48 h (Fig. 3C and D). Therefore, treating HepG2 cells with 2.5 μM

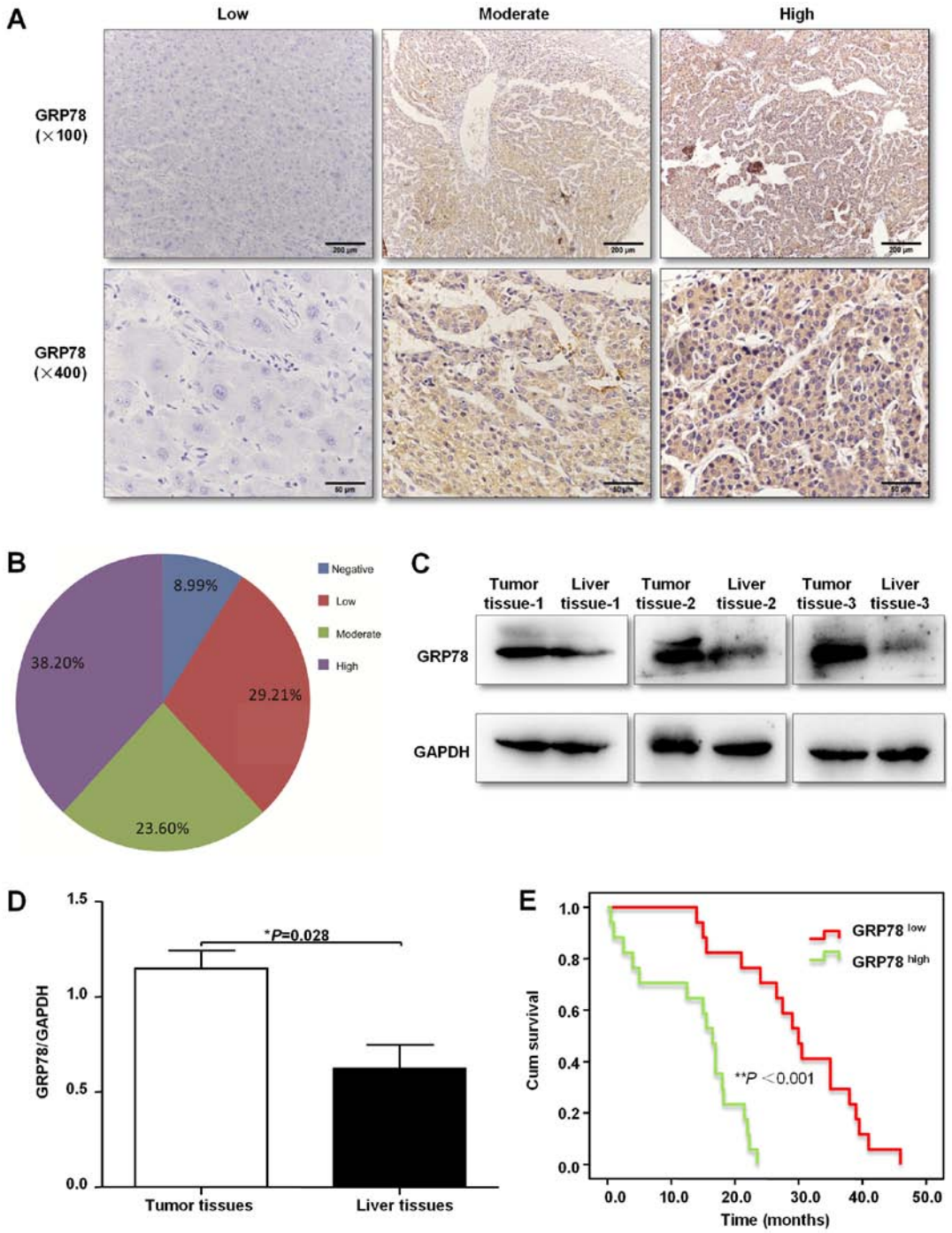

Figure 1. GRP78 expression is positively associated with poor prognosis in patients with liver cancer. (A) Representative images of the low, moderate and high expression levels of the ER stress marker protein GRP78 in liver cancer tissue samples. Magnifications, x100 for upper panel; x400 for lower panel. (B) Percentage of liver cancer tissues of negative, low, moderate and high expression levels of GRP78. (C) Western blot analysis of GRP78 protein expression in three human liver cancer tissue samples, and (D) semi-quantitative analysis of band intensity using Scion Image 4.0.3.2 relative to GAPDH intensity. (E) Kaplan-Meier curves of overall survival in patients stratified into high- and low-GRP78 expression groups. GRP78, glucose-regulated protein 78; ER, endoplasmic reticulum; Cum survival, cumulative survival.

TM for 24 h was considered the optical conditions to induce ER stress in subsequent experiments.

To physically characterize exosomes secreted from HepG2 cells, exosomes were isolated from the conditioned media of TM-treated cells. The purified pellets were imaged using TEM, and double-membrane structure vesicles that were within the expected diameter range of exosomes (30-100 nm) were observed (Fig. 3E). Furthermore, the presence of CD63 and TSG101, two specific exosomal markers, was observed, and the negative control, calnexin, was not identified in exosomes (Fig. 3F). Thus, the results suggest that the purified isolated pellets were exosomes.

Tumor cells can modulate the function of neighboring or distant cells via exosome-mediated delivery of molecules to recipient cells (20). To assess whether ER-stressed liver cancer cells modulated the role of macrophages via exosomes, RAW264.7 cells were cultured with PKH67-labeled exosomes, and the labeled exosomes were observed to be taken up by

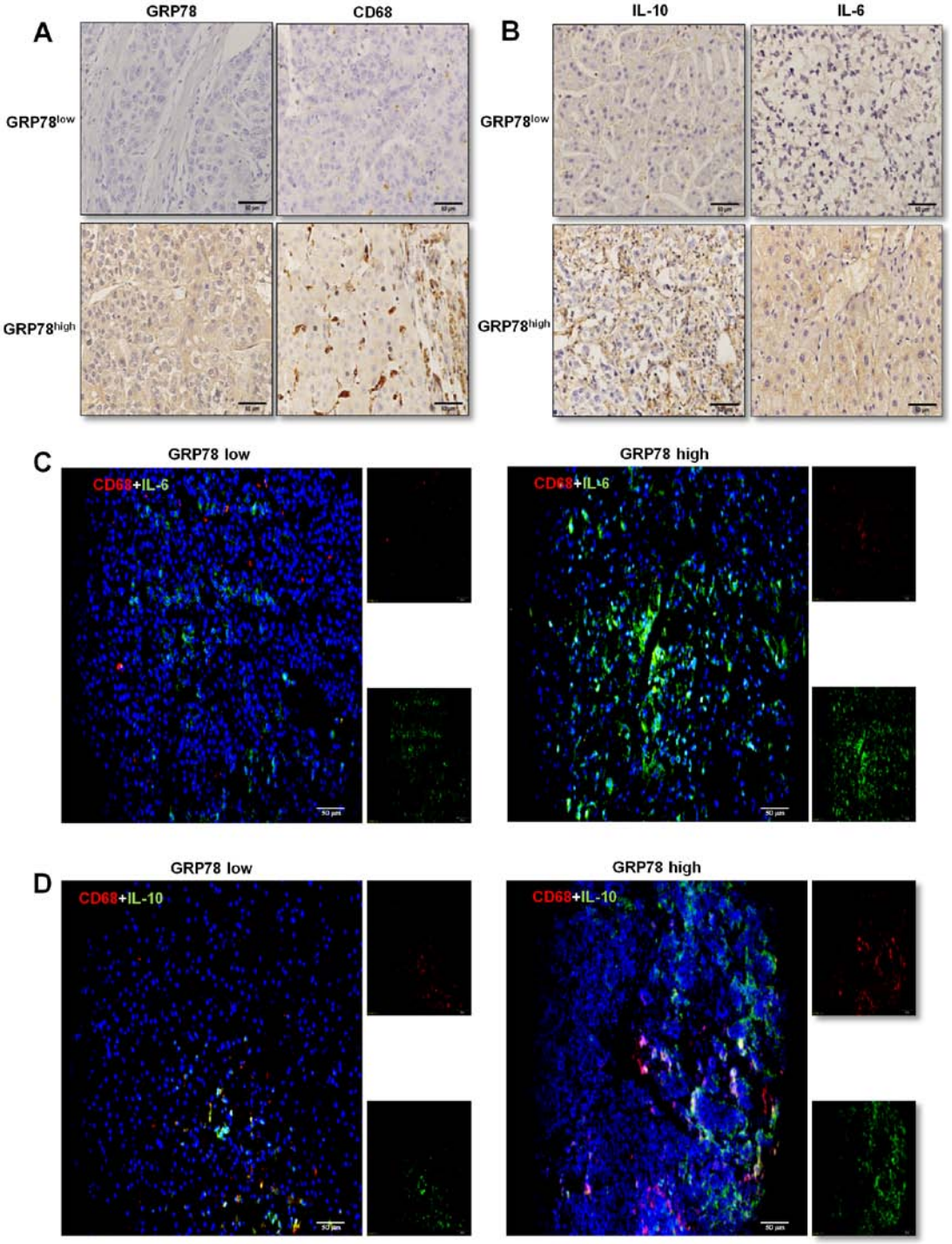

Figure 2. Upregulation of GRP78 is associated with macrophage infiltration and an inflammatory microenvironment in liver cancer. (A) Representative images of CD68 protein expression in $GRP78^{high}$ or $GRP78^{low}$ liver cancer tissues. (B) Representative images of IL-6 and IL-10 expression levels in liver cancer tissues with $GRP78^{high}$ or $GRP78^{low}$ expression levels. Immunofluorescence was used to measure the expression pattern of IL-6 (C) and IL-10 (D) in $CD68^{+}$ cells in GRP78-positive liver cancer tissues. Scale bar, 50 μm. GRP78, glucose-regulated protein 78; IL, interleukin.

RAW264.7 macrophages (Fig. 4A). To determine the effect of ER stress-associated exosomes on RAW264.7 cell immune function, cells were incubated with Exo-con and Exo-TM, and the levels of IL-6, MCP-1, IL-10 and TNF-α were detected using a CBA inflammatory cytokine kit. The results indicated that IL-6 (Fig. 4B; $P<0.05$), IL-10 (Fig. 4C; $P<0.05$) and MCP-1 (Fig. 4D; $P<0.01$) levels were significantly increased in Exo-TM treated cells, while the levels of TNF-α (Fig. 4E; $P>0.05$) were slightly decreased in Exo-TM treated RAW264.7 cells compared with Exo-con treated cells. Collectively, the results suggest that exosomes released from ER-stressed HepG2 cells influence the expression profile of cytokines secreted by macrophages.

ER stress-associated exosomes enhance cytokines expression by activating the STAT3 pathway. The underlying mechanism via which ER stress-associated exosomes affects cytokine expression in macrophages was subsequently

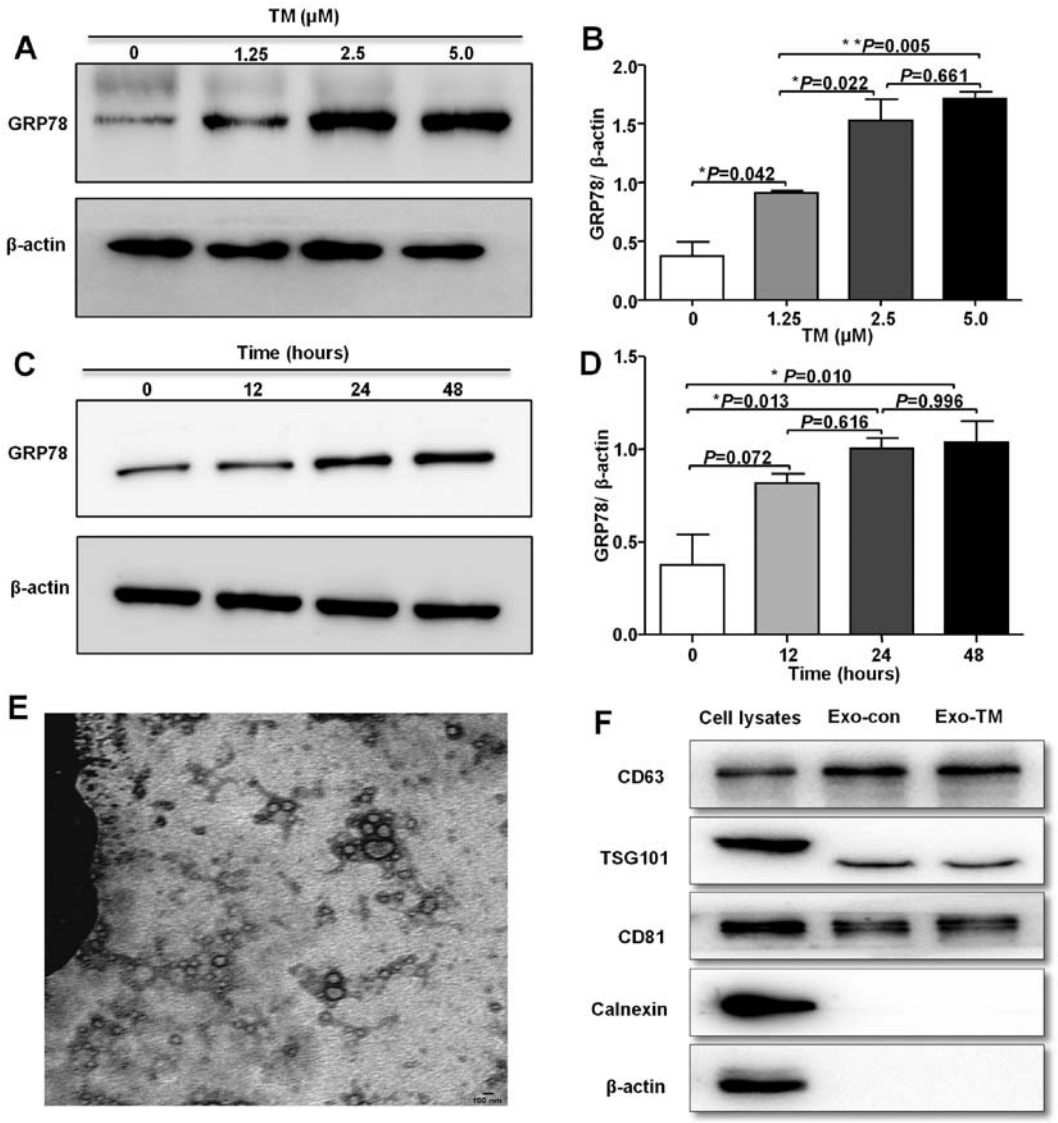

Figure 3. Characteristics of ER stress-associated exosomes. (A) HepG2 cells were treated with 0, 1.25, 2.5 and 5 μM TM for 24 h, and (B) GRP78 protein expression was measured and semi-quantitatively analyzed, relative to β-actin intensity. (C) HepG2 cells were treated with 2.5 μM TM for 12, 24 and 48 h, and (D) GRP78 protein expression was measured and semi-quantitatively analyzed, relative to β-actin intensity. (E) Representative transmission electron microscope images of Exo-TM. Scale bar, 100 nm. (F) Expression levels of CD63, TSG101, CD81, β-actin and Calnexin were measured using cell lysates or exosomes by western blotting. *P< 0.05, **P< 0.01. ER, endoplasmic reticulum; TM, tuniamycin; GRP78, glucose-regulated protein 78; Exo-TM, exosomes from the supernatants of HepG2 cells treated with 2.5 μM tunicamycin; TSG101, tumor susceptibility gene 101; Exo-con, exosomes from the supernatants of control HepG2 cells.

examined. The JAK2/STAT3 signaling pathway plays a vital role in the macrophage inflammatory response (21); therefore, whether the Exo-TM-mediated inflammatory response is JAK2/STAT3-dependent was investigated. It was found that Exo-TM significantly increased the protein expression levels of both p-JAK2 (P<0.05) and p-STAT3 (P<0.05; Fig. 5A-C). Furthermore, inhibition of STAT3 activation, using a selective STAT3 inhibitor (100 μM S3I-201; MedChemExpres) at 37˚C for 24 h, significantly decreased the Exo-TM-induced increase in p-STAT3 expression (Fig. 5D and E; P<0.05), but only slightly decreased p-JAK2 expression (Fig. 5D and F; P>0.05).

The results also demonstrated that inhibition of STAT3 abrogated Exo-con- and Exo-TM-induced elevation of IL-6 (Fig. 6A; P<0.05), IL-10 (Fig. 6B; P<0.05) and MCP-1 (Fig. 6C; P<0.01) levels secreted by RAW264.7 cells; however, inhibition of STAT3 did not affect TNF-α levels (Fig. 6D; P>0.05). Therefore, the results suggested that ER stress-associated exosomes increased the levels of IL-6, MCP-1 and IL-10 in macrophages via the JAK2/STAT3 signaling pathway.

Discussion

Primary liver cancer is one of the most common types of malignancies (1,2). Moreover, surgical resection is the primary treatment method for patients with early stage of liver cancer (2). However, due to the asymptomatic nature of the early stage of liver cancer, it is frequently diagnosed at the later stages, at which point surgery may not be suitable (2). Therefore, understanding the causes and mechanisms of drug resistance in liver cancer may improve the effects of chemotherapy on liver cancer, and thus, increase survival.

Systemic chemotherapy and target therapy are the two most frequently used treatment strategies for unresectable

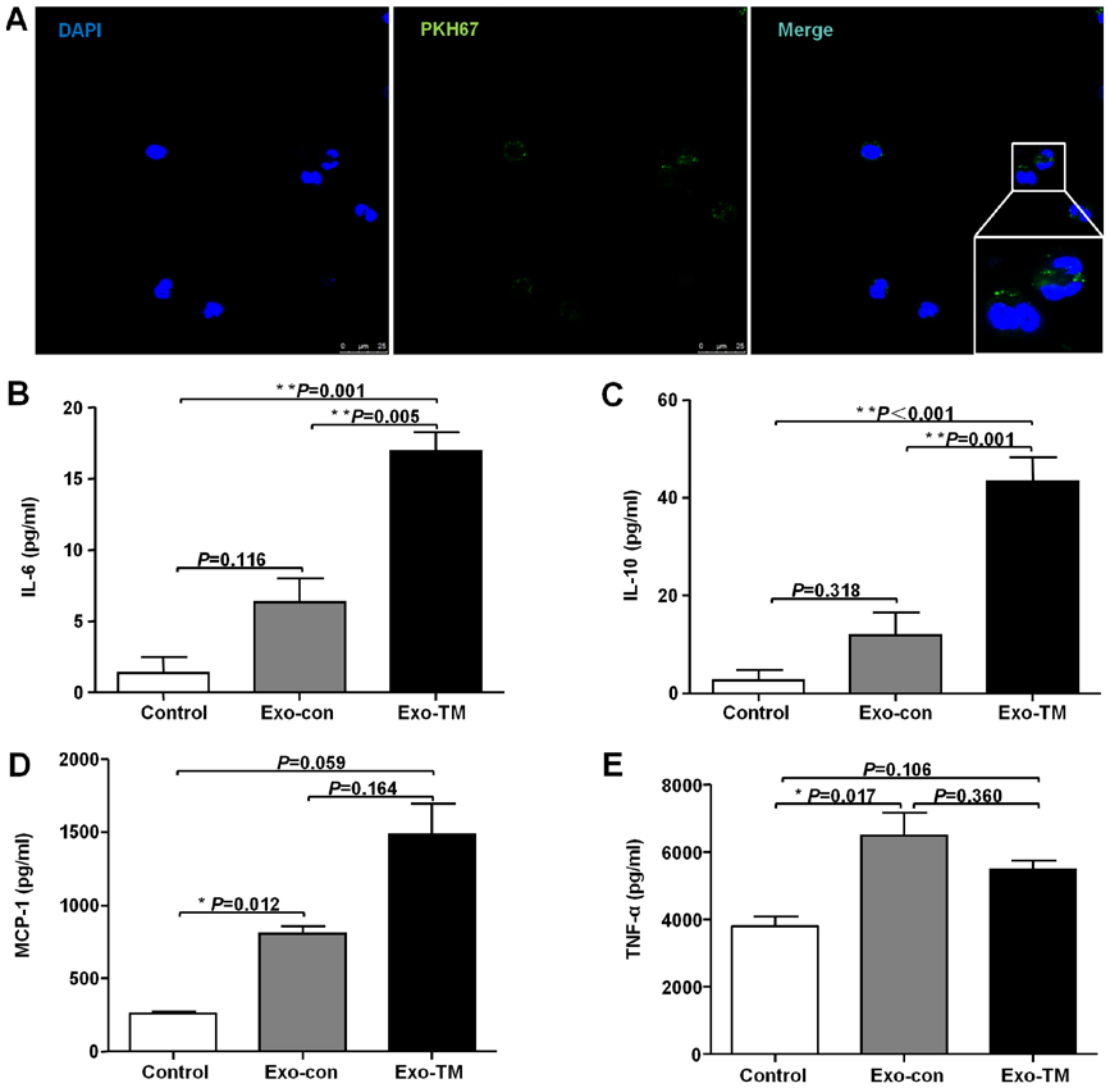

Figure 4. Incubation with Exo-TM increases expression of cytokines in macrophages *in vitro*. (A) Confocal microscopy was used to measure the incorporation of PKH67-labeled exosomes into RAW264.7 cells. Cells were incubated with Exo-con and Exo-TM for 24 h, and (B) IL-6, (C) IL-10, (D) MCP-1 and (E) TNF-α levels were measured using a CBA inflammatory factor kit. *P< 0.05, **P< 0.01 with indicated groups. Exo-Con, exosomes from the supernatants of control HepG2 cells; Exo-TM, exosomes from the supernatants of HepG2 cells treated with 2.5 μM tunicamycin; IL, interleukin; MCP-1, monocyte chemotactic protein-1; TNF-α, tumor necrosis factor-α; CBA, cytokine bead array.

and advanced liver cancer; however, these only improve OS modestly compared with best supportive care, due to drug resistance (22,23). Thus, novel treatment regimens are required to prolong survival. Escaping immune surveillance is one of the hallmarks of cancer (24,25), and investigating the specific molecular mechanisms involved in the modulation of immune escape in liver cancer cells may identify potential therapeutic target for clinical treatment of liver cancer.

Alterations in the TME, such as Ca^{2+} balance disorders, hypoxia and protein glycosylation inhibition, result in aberrant accumulation of misfolded or unfolded proteins in the ER, which cause ER stress to maintain homeostasis (4). Continuous activation of ER stress is a symbolic trait in a number of cancer types, including liver cancer (26,27), and serves a vital role in maintaining homeostasis via the activation of the three unfolded protein response (UPR) branches (28). In the present study, it was identified that 61.8% (55/89) of liver cancer tissues stained positively for GRP78, and activation of ER stress was correlated with inflammation and aggressive disease characteristics in patients with liver cancer. Moreover, a previous study showed that several ER stress-associated genes, such as PKR-like ER kinase, activating transcription factor 6 and inositol essential enzyme 1α were upregulated in HCC tissues (18). However, the precise function of ER stress in shaping the TME and the anti-tumor immune response has not been previously examined. ER stress has been reported to induce inflammatory responses, and numerous ER stress-associated diseases also exhibit inflammatory phenotypes (29). Furthermore, ER stress-associated inflammation is necessary for tissue remodeling, which contributes to tissue injury and serves an important role in promoting the development of a variety of inflammation-associated diseases (30). It has also been shown that ER-stressed tumor cells can either directly induce inflammation, via the UPR pathway, or indirectly interact with innate immune cells.

Cytokines released by ER-stressed tumor cells may act as warning signals for non-tumor cells (31). Chronic

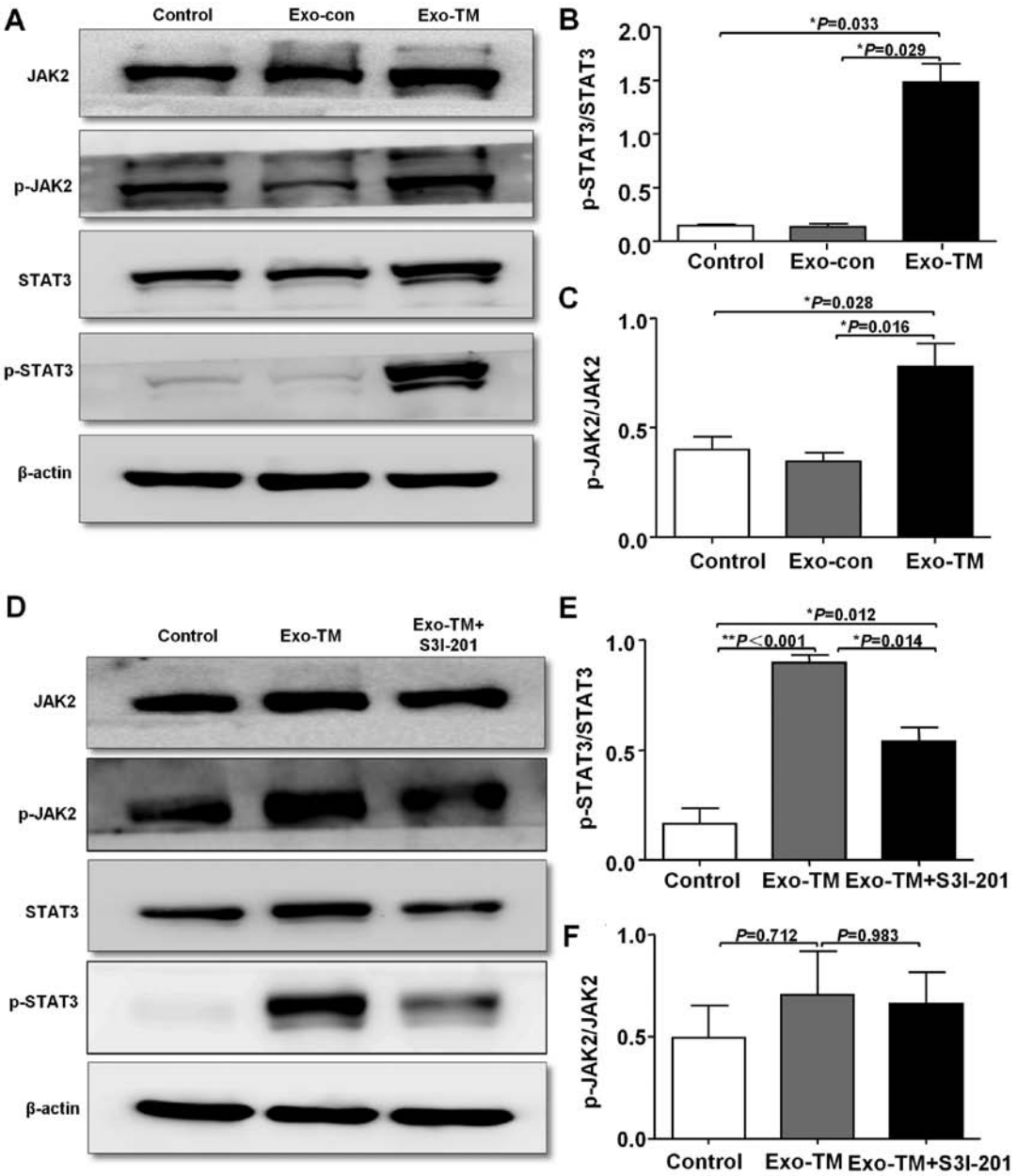

Figure 5. Exo-TM enhances cytokine expression by activating the JAK2/STAT3 pathway. RAW264.7 cells were treated with Exo-con or Exo-TM for 24 h. (A) Protein expression levels of the JAK2/STAT3 pathway were measured by western blot analysis. Blots presented in (A) were semi-quantitatively analyzed for comparing the (B) p-STAT3/STAT3 and (C) p-JAK2/JAK2 ratios, relative to β-actin intensity. (D) Western blot analysis of the protein expression levels of members of the JAK2/STAT3 signaling pathway in RAW264.7 cells treated with Exo-TM and S3I-201. Blots presented in (D) were semi-quantitatively analyzed for comparing the (E) p-STAT3/STAT3 and (F) p-JAK2/JAK2 ratios, relative to β-actin intensity. *P< 0.05, **P< 0.01 with indicated groups. Exo-Con, exosomes from the supernatants of control HepG2 cells; Exo-TM, exosomes from the supernatants of HepG2 cells treated with 2.5 μM tunicamycin; TM, tunicamycin; JAK2, Janus kinase 2; p-, phosphorylated.

inflammation is involved at various stages of promoting tumor progression, via a number of different mechanisms (32,33). For example, chronic inflammation may promote the production of tumor-promoting cytokines from tumor cells or tumor-associated immune cells, via the NF-κB and STAT3 signaling pathways (32,33). TAMs have also been reported to express additional cytokines, such as TNF-α, IL-6 and IL-10 (34). IL-6 is a potent driver of tumor growth and metastasis in several tumor models and can protect against apoptosis via the activation of STAT3 in a hypoxic microenvironment (35). Furthermore, IL-10 is the primary anti-inflammatory factor secreted by TAMs, which promotes tumor progression by enhancing tumor cell proliferation, invasion, stimulating tumor angiogenesis and inhibiting the anti-tumor immune response (36). MCP-1 is a small cytokine belonging to the CC chemokine family, which has specific chemotactic activation effect on monocytes and macrophages (37). Previous studies have shown that MCP-1 is an important pro-inflammatory cytokine that helps to recruit TAMs in TME (38). TAMs also secreted TNF-α to promote epithelial-mesenchymal transition and cancer stemness (39). Moreover, inflammation promotes tumor progression by inhibiting cell apoptosis and activating angiogenesis (40,41). In the present study, it was found that GRP78 expression was positively associated with CD68,

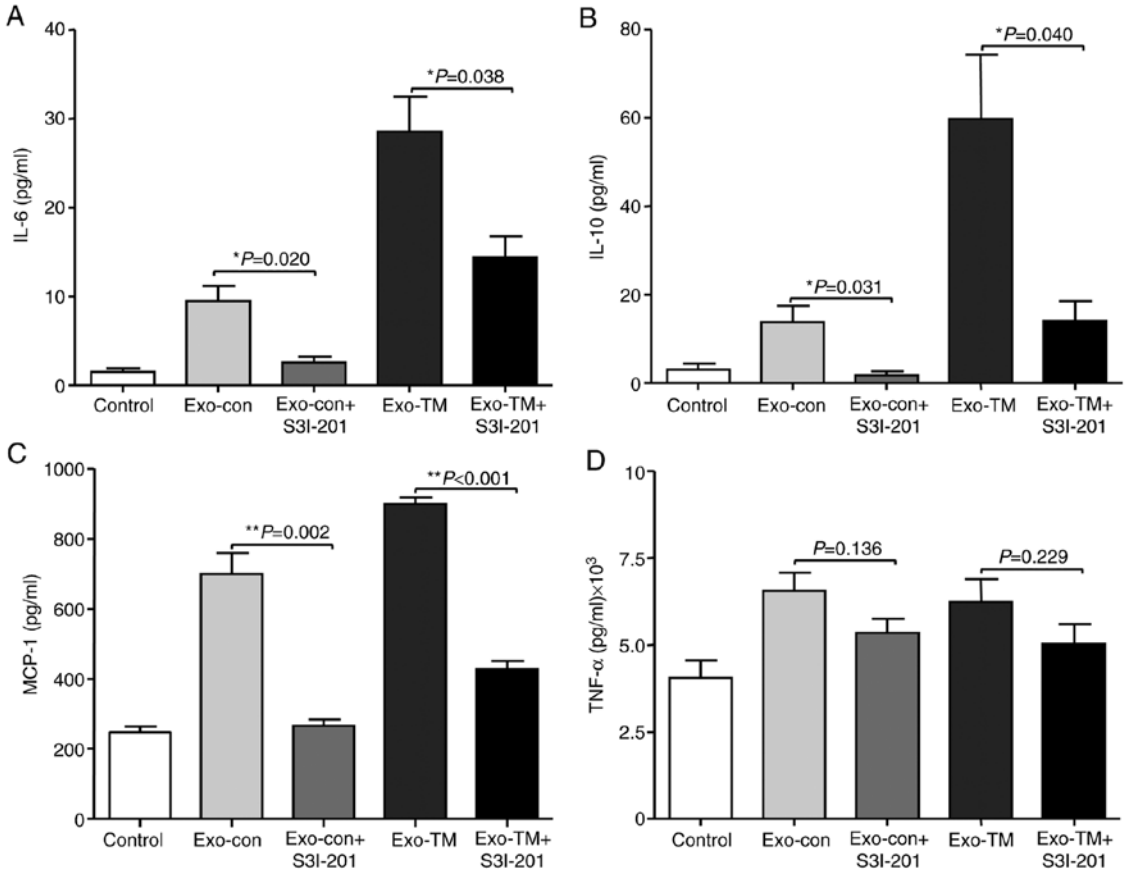

Figure 6. Inhibition of STAT3 decreases Exo-TM-induced cytokine expression. RAW264.7 macrophages were treated with Exo-con or Exo-TM with or without S3I-201 for 24 h. (A) IL-6, (B) IL-10, (C) MCP-1 and (D) TNF-α levels were measured using a CBA inflammatory factor kit. *P< 0.05, **P< 0.01 with indicated groups. Exo-Con, exosomes from the supernatants of control HepG2 cells; Exo-TM, exosomes from the supernatants of HepG2 cells treated with 2.5 μM tunicamycin; IL, interleukin; MCP-1, monocyte chemotactic protein-1; TNF-α, tumor necrosis factor-α; CBA, cytokine bead array.

IL-10 and IL-6 levels. In addition, protein expression levels of IL-10 and IL-6 in CD68$^+$ TAMs were increased in the GRP78-positive liver cancer tissues, which was consistent with a previous study (18). Therefore, the present results suggested that ER stress plays an important role in hampering anti-tumor immunity in liver cancer cells. However, the mechanism via which ER stress exerts modulation of the TME, and thus remodeling the anti-tumor effect of immune cells to promote tumor progression, remains unknown.

Exosomes play a critical role in intercellular communication by delivering their contents, such as proteins, DNA and miRNA, to cells in local microenvironments or distant target cells (14,42). In the present study, it was hypothesized that exosomes may transmit ER stress-associated signals to macrophages and modulate their function. In the present study, purified exosomes were labeled with PKH67 and it was found that RAW264.7 cells effectively engulfed the labeled exosomes released by HepG2 cells. Moreover, ER-stressed liver cancer cells released exosomes, which significantly increased the levels of IL-6, IL-10 and MCP-1, and slightly increased TNF-α levels. It was also demonstrated that treatment of cells with Exo-TM for 24 h activated the JAK2/STAT3 signaling pathway, which has an important role in inflammation response and liver cancer progression (43). The contents of exosomes are very complex; currently, >10,000 proteins, 200 lipids, 2,000 mRNAs and ~1,000 micro(mi)RNAs have been reported to be present in exosomes secreted by different cells (44). In a previous study, exosomes derived from ER-stressed liver cancer cells transmitted miRNA-23a-3p to macrophages resulting in the upregulation of programmed death-ligand 1 expression in macrophages (18). However, transfection of macrophages with either miRNA-23a-3p mimics or inhibitor did not affect the secretion of cytokines, such as IL-10 and IL-6 (data not shown). Thus, the precise mechanism contributing to the upregulation of cytokine secretion by ER stress-associated exosomes requires further investigation.

STAT3 not only plays an indispensable role in early embryonic development and differentiation of bone marrow cells, but also participates in the regulation of physiological functions such as tumor growth, differentiation, angiogenesis, invasion, metastasis and immune escape (45). Furthermore, the activation of STAT3 is an established pathway that mediates the inflammatory immune response in response to cytokine signals (46,47). To investigate whether STAT3 was involved in Exo-TM-induced inflammation, the expression of p-STAT3 in RAW264.7 treated with Exo-TM was determined, and it was found that p-STAT3 expression was increased in cells treated with Exo-TM for 24 h. Furthermore, inhibition of STAT3 using S3I-201 significantly reduced p-STAT3 expression in cells and decreased the levels of MCP-1, IL-6 and IL-10. Collectively, the present

results suggest that activation of the JAK2/STAT3 pathway may be a potential mechanism, via which exosomes secreted by ER-stressed liver cancer cells mediate the inflammatory response. S3I-201 not only inhibits STAT3-STAT3 complex formation, STAT3-DNA binding and transcriptional activities, but also inhibits STAT1 and STAT5 (48). Thus, STAT1 and STAT5 may be also involved in S3I-201-induced cytokine expression reduction.

In conclusion, the present result suggested that ER-stressed liver cancer cells promoted cytokine expression via exosome-mediated activation of the JAK2/STAT3 pathway in macrophages, which resulted in immunosuppression of macrophages, thus facilitating tumor progression. Therefore, the present study identified the potential of targeting the exosomal-STAT3 signaling pathway to abrogate ER stress-associated immune suppression in liver cancer.

Acknowledgements

The authors would like to thank Professor Wei Wei and Professor Yujing Wu from the Institute of Clinical Pharmacology, Anhui Medical University (Hefei, China) for their technical assistance during the experimental stages of the present study.

Funding

The present study was funded by the National Natural Science Foundation of China (grant nos. 81572430 and 81872047).

Availability of data and materials

The datasets used and/or analyzed during the present study are available from the corresponding author upon reasonable request.

Authors' contributions

GS and HW designed the present study and drafted the initial manuscript. CH and LF performed the biological experiments. JL and WH analyzed the data, while JL critically revised the manuscript for important intellectual content. All authors have red and approved the manuscript.

Ethics approval and consent to participate

The protocol of the current study conforms to the Ethical Guidelines of the 1975 Declaration of Helsinki and was approved by the Ethics Committee of The First Affiliated Hospital of Anhui Medical University (approval no. 20040158). Written consent was provided by all the enrolled patients.

Patient consent for publication

Not applicable.

Competing interests

The authors declare that they have no competing interests.

References

1. Bray F, Ferlay J, Soerjomataram I, Siegel RL, Torre LA and Jemal A: Global cancer statistics 2018: GLOBOCAN estimates of incidence and mortality worldwide for 36 cancers in 185 countries. CA Cancer J Clin 68: 394-424, 2018.
2. Forner A, Reig M and Bruix J: Hepatocellular carcinoma. Lancet 391: 1301-1314, 2018.
3. Ringelhan M, Pfister D, O'Connor T, Pikarsky E and Heikenwalder M: The immunology of hepatocellular carcinoma. Nat Immunol 19: 222-232, 2018.
4. Cubillos-Ruiz JR, Bettigole SE and Glimcher LH: Tumorigenic and immunosuppressive effects of endoplasmic reticulum stress in cancer. Cell 168: 692-706, 2017.
5. Wang M, Law ME, Castellano RK and Law BK: The unfolded protein response as a target for anticancer therapeutics. Crit Rev Oncol Hematol 127: 66-79, 2018.
6. Hetz C and Papa FR: The unfolded protein response and cell fate control. Mol Cell 69: 169-181, 2018.
7. Shen K, Johnson DW, Vesey DA, McGuckin MA and Gobe GC: Role of the unfolded protein response in determining the fate of tumor cells and the promise of multi-targeted therapies. Cell Stress Chaperones 23: 317-334, 2018.
8. Rubio-Patiño C, Bossowski JP, Chevet E and Ricci JE: Reshaping the immune tumor microenvironment through IRE1 signaling. Trends Mol Med 24: 607-614, 2018.
9. Yoo YS, Han HG and Jeon YJ: Unfolded protein response of the endoplasmic reticulum in tumor progression and immunogenicity. Oxid Med Cell Longev 2017: 2969271, 2017.
10. Rufo N, Garg AD and Agostinis P: The unfolded protein response in immunogenic cell death and cancer immunotherapy. Trends Cancer 3: 643-658, 2017.
11. Seelige R, Searles S and Bui JD: Mechanisms regulating immune surveillance of cellular stress in cancer. Cell Mol Life Sci 75: 225-240, 2018.
12. Ye L, Zhang Q, Cheng Y, Chen X, Wang G, Shi M, Zhang T, Cao Y, Pan H, Zhang L, *et al*: Tumor-derived exosomal HMGB1 fosters hepatocellular carcinoma immune evasion by promoting TIM-1+ regulatory B cell expansion. J Immunother Cancer 6: 145, 2018.
13. Jella KK, Nasti TH, Li Z, Malla SR, Buchwald ZS and Khan MK: Exosomes, their biogenesis and role in inter-cellular communication, tumor microenvironment and cancer immunotherapy. Vaccines (Basel) 6: pii: E69, 2018.
14. Hu C, Chen M, Jiang R, Guo Y, Wu M and Zhang X: Exosome-related tumor microenvironment. J Cancer 9: 3084-3092, 2018.
15. Li X, Wang Y, Wang Q, Liu Y, Bao W and Wu S: Exosomes in cancer: Small transporters with big functions. Cancer Lett 435: 55-65, 2018.
16. Chen X, Zhou J, Li X, Wang X, Lin Y and Wang X: Exosomes derived from hypoxic epithelial ovarian cancer cells deliver microRNAs to macrophages and elicit a tumor-promoted phenotype. Cancer Lett 435: 80-91, 2018.
17. Seo N, Akiyoshi K and Shiku H: Exosome-mediated regulation of tumor immunology. Cancer Sci 109: 2998-3004, 2018.
18. Liu J, Fan L, Yu H, Zhang J, He Y, Feng D, Wang F, Li X, Liu Q, Li Y, *et al*: Endoplasmic reticulum stress causes liver cancer cells to release exosomal miR-23a-3p and up-regulate programmed death ligand 1 expression in macrophages. Hepatology 70: 241-258, 2019.
19. Noy R and Pollard JW: Tumor-associated macrophages: From mechanisms to therapy. Immunity 41: 49-61, 2014.
20. Huang Y, Liu K, Li Q, Yao Y and Wang Y: Exosomes function in tumor immune microenvironment. Adv Exp Med Biol 1056: 109-122, 2018.
21. Cui J, Zhang F, Cao W, Wang Y, Liu J, Liu X, Chen T, Li L, Tian J and Yu B: Erythropoietin alleviates hyperglycaemia-associated inflammation by regulating macrophage polarization via the JAK2/STAT3 signalling pathway. Mol Immunol 101: 221-228, 2018.
22. Kudo M: Systemic therapy for hepatocellular carcinoma: Latest advances. Cancers (Basel) 10: pii: E412, 2018.
23. Kulik L and El-Serag HB: Epidemiology and management of hepatocellular carcinoma. Gastroenterology 156: 477-491.e1, 2019.
24. Lapitz A, Arbelaiz A, Olaizola P, Aranburu A, Bujanda L, Perugorria MJ and Banales JM: Extracellular vesicles in hepatobiliary malignancies. Front Immunol 9: 2270, 2018.

25. da Motta Girardi D, Correa TS, Crosara Teixeira M and Dos Santos Fernandes G: Hepatocellular carcinoma: Review of targeted and immune therapies. J Gastrointest Cancer 49: 227-236, 2018.
26. Roth GS and Decaens T: Liver immunotolerance and hepatocellular carcinoma: Patho-physiological mechanisms and therapeutic perspectives. Eur J Cancer 87: 101-112, 2017.
27. Banerjee S and Zhang W: Endoplasmic reticulum: Target for next-generation cancer therapy. Chembiochem 19: 2341-2343, 2018.
28. Corazzari M, Gagliardi M, Fimia GM and Piacentini M: Endoplasmic reticulum stress, unfolded protein response, and cancer cell fate. Front Oncol 7: 78, 2017.
29. Osorio F, Tavernier SJ, Hoffmann E, Saeys Y, Martens L, Vetters J, Delrue I, De Rycke R, Parthoens E, Pouliot P, *et al*: The unfolded-protein-response sensor IRE-1α regulates the function of CD8α+ dendritic cells. Nat Immunol 15: 248-257, 2014.
30. Garg AD, Kaczmarek A, Krysko O, Vandenabeele P, Krysko DV and Agostinis P: ER stress-induced inflammation: Does it aid or impede disease progression? Trends Mol Med 18: 589-598, 2012.
31. Grootjans J, Kaser A, Kaufman RJ and Blumberg RS: The unfolded protein response in immunity and inflammation. Nat Rev Immunol 16: 469-484, 2016.
32. Räihä MR and Puolakkainen PA: Tumor-associated macrophages (TAMs) as biomarkers for gastric cancer: A review. Chronic Dis Transl Med 4: 156-163, 2018.
33. Chen W, Jiang J, Xia W and Huang J: Tumor-related exosomes contribute to tumor-promoting microenvironment: An immunological perspective. J Immunol Res 2017: 1073947, 2017.
34. Zhang X, Zeng Y, Qu Q, Zhu J, Liu Z, Ning W, Zeng H, Zhang N, Du W, Chen C and sHuang JA: PD-L1 induced by IFN-γ from tumor-associated macrophages via the JAK/STAT3 and PI3K/AKT signaling pathways promoted progression of lung cancer. Int J Clin Oncol 22: 1026-1033, 2017.
35. Jeong SK, Kim JS, Lee CG, Park YS, Kim SD, Yoon SO, Han DH, Lee KY, Jeong MH and Jo WS: Tumor associated macrophages provide the survival resistance of tumor cells to hypoxic microenvironmental condition through IL-6 receptor-mediated signals. Immunobiology 222: 55-65, 2017.
36. Ruffell B, Chang-Strachan D, Chan V, Rosenbusch A, Ho CM, Pryer N, Daniel D, Hwang ES, Rugo HS and Coussens LM: Macrophage IL-10 blocks CD8+ T cell-dependent responses to chemotherapy by suppressing IL-12 expression in intratumoral dendritic cells. Cancer Cell 26: 623-637, 2014.
37. Ibi M, Horie S, Kyakumoto S, Chosa N, Yoshida M, Kamo M, Ohtsuka M and Ishisaki A: Cell-cell interactions between monocytes/macrophages and synoviocyte-like cells promote inflammatory cell infiltration mediated by augmentation of MCP-1 production in temporomandibular joint. Biosci Rep 38: pii: BSR20171217, 2018.
38. Hultgren EM, Patrick ME, Evans RL, Stoos CT and Egland KA: SUSD2 promotes tumor-associated macrophage recruitment by increasing levels of MCP-1 in breast cancer. PLoS One 12: e0177089, 2017.
39. Chen Y, Wen H, Zhou C, Su Q, Lin Y, Xie Y, Huang Y, Qiu Q, Lin J, Huang X, *et al*: TNF-α derived from M2 tumor-associated macrophages promotes epithelial-mesenchymal transition and cancer stemness through the Wnt/β-catenin pathway in SMMC-7721 hepatocellular carcinoma cells. Exp Cell Res 378: 41-50, 2019.
40. Wu X, Tao P, Zhou Q, Li J, Yu Z, Wang X, Li J, Li C, Yan M, Zhu Z, *et al*: IL-6 secreted by cancer-associated fibroblasts promotes epithelial-mesenchymal transition and metastasis of gastric cancer via JAK2/STAT3 signaling pathway. Oncotarget 8: 20741-20750, 2017.
41. Zhao X, Fan W, Xu Z, Chen H, He Y, Yang G, Yang G, Hu H, Tang S, Wang P, *et al*: Inhibiting tumor necrosis factor-alpha diminishes desmoplasia and inflammation to overcome chemoresistance in pancreatic ductal adenocarcinoma. Oncotarget 7: 81110-81122, 2016.
42. Wan Z, Gao X, Dong Y, Zhao Y, Chen X, Yang G and Liu L: Exosome-mediated cell-cell communication in tumor progression. Am J Cancer Res 8: 1661-1673, 2018.
43. Ding YF, Wu ZH, Wei YJ, Shu L and Peng YR: Hepatic inflammation-fibrosis-cancer axis in the rat hepatocellular carcinoma induced by diethylnitrosamine. J Cancer Res Clin Oncol 143: 821-834, 2017.
44. Théry C, Witwer KW, Aikawa E, Alcaraz MJ, Anderson JD, Andriantsitohaina R, Antoniou A, Arab T, Archer F, Atkin-Smith GK, *et al*: Minimal information for studies of extracellular vesicles 2018 (MISEV2018): A position statement of the international society for extracellular vesicles and update of the MISEV2014 guidelines. J Extracell Vesicles 7: 1535750, 2018.
45. Belmokhtar K, Bourguignon T, Worou ME, Khamis G, Bonnet P, Domenech J and Eder V: Regeneration of three layers vascular wall by using BMP2-treated MSC involving HIF-1α and Id1 expressions through JAK/STAT pathways. Stem Cell Rev Rep 7: 847-859, 2011.
46. Laudisi F, Cherubini F, Monteleone G and Stolfi C: STAT3 Interactors as potential therapeutic targets for cancer treatment. Int J Mol Sci 19: pii: E1787, 2018.
47. Wang Y, Shen Y, Wang S, Shen Q and Zhou X: The role of STAT3 in leading the crosstalk between human cancers and the immune system. Cancer Lett 415: 117-128, 2018.
48. Siddiquee K, Zhang S, Guida WC, Blaskovich MA, Greedy B, Lawrence HR, Yip ML, Jove R, McLaughlin MM, Lawrence NJ, *et al*: Selective chemical probe inhibitor of Stat3, identified through structure-based virtual screening, induces antitumor activity. Proc Natl Acad Sci USA 104: 7391-7396, 2007.